

SUPPORTING INFORMATION

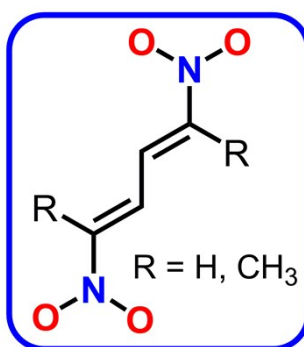
π -Hole interactions at work: crystal engineering with nitro-derivatives

Antonio Bauzá,^a Anastasiya V. Sharko,^b Ganna A. Senchyk,^b Eduard B. Rusanov,^c Antonio Frontera,^{a,*} and Kostiantyn V. Domasevitch^{b,*}

^a *Departament de Química, Universitat de les Illes Balears, Crta de Valldemossa km 7.5, 07122 Palma de Mallorca (Balears), Spain*

^b *Inorganic Chemistry Dpt, Taras Shevchenko National University of Kyiv, Volodymyrska Str. 64/13, Kyiv 01601, Ukraine. E-mail: dk@univ.kiev.ua*

^c *Institute of Organic Chemistry, Murmanska Str.4, Kyiv 253660, Ukraine*



CONTENTS

1. Organic synthesis.....	2
2. Crystallography.....	5
3. Details for Crystal structures of the Dinitrodienes.....	5
3.1. Structure of 1,4-Dinitrobutadiene (1).....	5
3.2. Structure of 1,4-Dinitro-1,3-butadiene 1,4-dioxane solvate (1a).....	7
3.3. Structure of 1,4-Dinitro-1,3-pentadiene (2).....	9
3.4. Structure of 2,4-Dinitro-2,4-hexadiene (3).....	12
3.5. Computational methods.....	14

1. Organic synthesis

CAUTION:

The aliphatic nitro compounds are potentially explosive. A great care should be addressed to the maintaining bath temperature below 50-60°C, during vacuum concentrations of the reaction mixtures.

“1,4-dinitro-1,3-butadiene can be caused to explode forcefully when heated in a closed container or when detonated by a blasting cap; accordingly, due precaution should be taken when this and related compounds are handled” [1a].

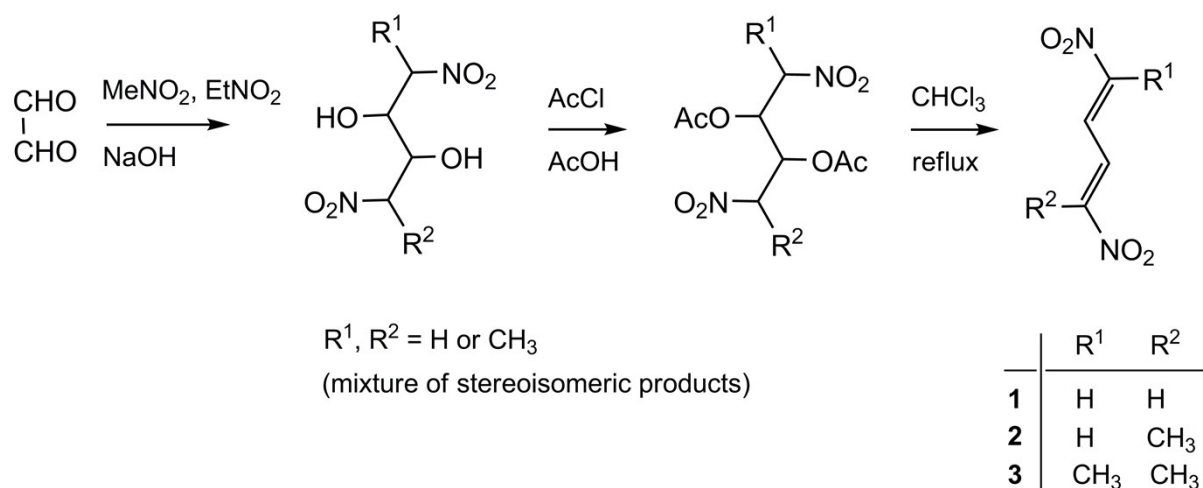
1.1. Synthesis of 1,4-dinitro-1,3-butadiene (1) and 2,5-dinitro-2,4-hexadiene (3)

All the chemicals were commercial products (Acros) of reagent grade, used without further purification. NMR spectra were recorded on a Bruker 400 MHz spectrometer.

The compounds were prepared by the literature three-step procedures involving alkali-mediated condensation of glyoxal and nitromethane [1] or nitroethane [2], acylation of the dinitrodiols with acetyl chloride and subsequent elimination of AcOH by reflux of chloroform solutions in the presence of catalytic amounts of KHCO_3 .

Single crystals of the compounds **1** and **3** were obtained by slow evaporation of ethyl acetate solutions. In the case of **1**, slow evaporation of solution in 1,4-dioxane led to crystallization of the adduct **1**·(1,4-Diox) as large light-yellow prisms. It readily loses solvent molecules when exposed to air.

1.2. Synthesis of 1,4-dinitropenta-1,3-diene (2)



Hitherto unknown 1,4-dinitropenta-1,3-diene (**2**) was prepared following reaction sequences for the 1,4-dinitro-1,3-butadiene (**1**) [1] and 2,5-dinitrohexa-2,4-diene (**3**) [2] analogs and starting with equimolar mixture of nitromethane and nitroethane. This reaction yields a mixture of numerous products: DL-pair and *meso*-form of 1,4-dinitro-2,3-butanediols ($R^1, R^2 = H$), four DL-pairs and two *meso*-forms of hexanediols ($R^1, R^2 = CH_3$), and even a larger number of isomeric pentanediols ($R^1 = H, R^2 = CH_3$). This complex mixture was used for the next steps without separation and characterization of the individual species. Final reaction product represents mixture of only three compounds, dinitrobuta- (**1**), penta- (**2**) and hexadienes (**3**). The target 1,4-dinitropenta-1,3-diene (**2**) is readily separable by fractional crystallization. This low-melting material is readily soluble in benzene or dichloromethane, unlike very sparingly soluble symmetric buta- and hexadienes.

61.0 mL of 40% aqueous glyoxal solution (0.53 mol) and solution 42.7 g NaOH in 65 mL of water were added dropwise, with two separate addition funnels, to a cold (bath temperature 0°C) well-stirred mixture of 141 mL (2.60 mol) nitromethane, 187 mL (2.60 mol) nitroethane and 370 mL methanol, for a period of 2 h. Then the stirring was continued for next hour at the same temperature. The mixture was diluted with 150 mL cold water and then saturated with sulfur dioxide by passing the gas through the solution and maintaining temperature below 15-20°C. Then 200 mL water was added and the organic layer was separated. This solution was evaporated with rotari evaporator and bath temperature below 60°C and the viscous residue was dried under vacuum (0.1 mm Hg) for 5 h.

This material was dissolved in 150 mL of glacial acetic acid and 120 mL of acetyl chloride was added dropwise for 10 min with stirring. When the initial extensive evolution of HCl gas ceased, the flask was placed into the pre-heated oil bath (85-90°C) and the mixture was vigorously stirred for 12 min. The resulting yellow solution was cooled to 30-40°C and the reaction product was precipitated as brown oil by addition of 0.4 L of ice water. This oil was separated by decantation, washed with 100 mL water and dried under vacuum (0.1 mm Hg) for 10 h. The obtained brown semisolid product was used in the next step without separation of individual compounds.

It was dissolved in 1 L of dry, acid-free chloroform, 1.0 g of finely powdered $KHCO_3$ was added and the mixture was vigorously refluxed under powerful stirring for 6 h. The resulting dark solution was filtered when cold and then evaporated to a volume of 50-60 mL under reduced pressure (bath temperature below 50-60°C). Brownish crystalline product was separated, washed with 10 ml of cold chloroform and dried in air. This material was dissolved in boiling benzene, the solution was filtered, evaporated to a half of the initial volume under reduced

pressure and cooled to 5-10°C. Yellow crystalline deposit, consisting of sparingly soluble symmetric 1,4-dinitro-1,3-butadiene (major) and 2,5-dinitro-2,4-hexadiene, was filtered off and discarded. The filtrate was evaporated under reduced pressure giving light-yellow oil, which crystallized when cold. The yield was 22.7 g (27% based on glyoxal used). Single crystals of the compound were obtained by slow evaporation of methanol solution. Solutions in alcohols darken, while essential stabilization occurs with traces of acetic acid.

1,4-Dinitropenta-1,3-diene (2), yellow crystals, mp = 72°C (benzene).

Elemental analysis calcd for C₅H₆N₂O₄: C 37.98, H, 3.82, N 17.72; found: C 38.25, H 3.80, N 17.51%.

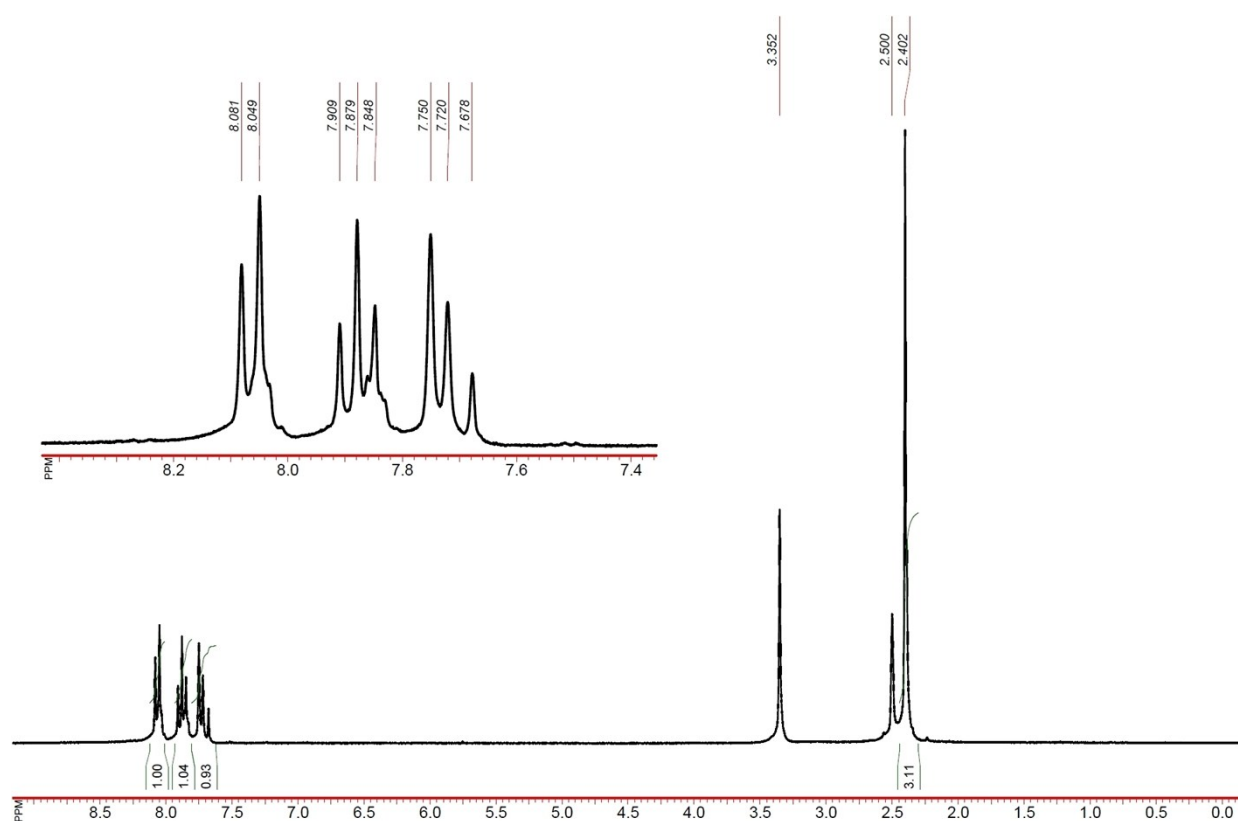


Figure S1. NMR ¹H spectrum of 1,4-dinitropenta-1,3-diene (2) (dmsO-d₆, Bruker 400 MHz)

[1] (a) F. I. Carrol, *J. Org. Chem.* **1966**, 31, 366; (b) S. S. Novikov, I. S. Korsakova and K. K. Babivskii, *Bull. Acad. Sci. USSR Div. Chem. Sci.* (Engl. Transl.) **1960**, 882–884.

[2] A.V. Sharko, G.A. Senchyk, E.B. Rusanov and K.V. Domasevitch, *Tetrahedron Lett.* **2015**, 56, 6089-6092.

2. Crystallography

The diffraction data were collected with graphite-monochromated Mo K α radiation ($\lambda = 0.71073$ Å). Measurements for **1a** and **2** at 213K were made using a Stoe Image Plate Diffraction System, ϕ oscillation scans (ϕ 0 \rightarrow 180 $^\circ$; $\Delta\phi = 0.9^\circ$; exposure times 8-10 min per frame).^[1] Measurements for **1** and **3** were performed at 293 K on a Bruker APEXII CCD area-detector diffractometer (ω scans). The data were corrected for Lorentz-polarization effects and for the effects of absorption (multi-scans method). The structures were solved by direct methods and refined by full-matrix least-squares on F^2 using the SHELX-97 package.^[2] All the CH-hydrogen atoms were located and freely refined with isotropic thermal parameters.

[1] (a) Stoe & Cie. X-SHAPE. Revision 1.06, Stoe & Cie GmbH, Darmstadt, Germany, **1999**; (b) Stoe & Cie. X-RED. Version 1.22, Stoe & Cie GmbH, Darmstadt, Germany, **2001**.

[2] (a) Sheldrick, G. M. *Acta Crystallogr.* **1990**, *A46*, 467; (b) Sheldrick, G. M. *Acta Crystallogr.* **2008**, *A64*, 112.

3. Details for Crystal structures of the Dinitrodienes

3.1. Structure of 1,4-Dinitrobutadiene (**1**)

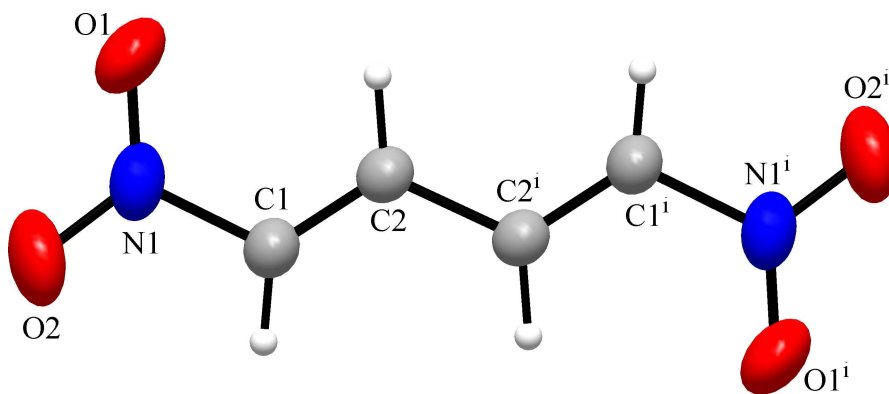


Figure S2. Molecular structure of **1**, with the thermal ellipsoids at 45% probability level. Symmetry code: (i) $-x, -y, -z$.

In the crystal, molecules of 1,4-dinitrobutadiene adopt centrosymmetric *trans-trans*-configuration and reside across a center of inversion. Primary intermolecular interactions in the structure are provided by a set of “double” CH \cdots O bonds between pairs of 1,3-CH and nitro groups, which assemble the molecules into 2D square nets. One of the CH hydrogen bonds is

bifurcate and the second, slightly weaker, branch is established between the layers: C1-H1...O2^{vi} (1-x, -y, 1-z) = 3.428(2) Å.

Table S1. Hydrogen-bond geometry (Å, °) for structure of **1**.

Donor (D)	Hydrogen (H)	Acceptor (A) ^{a)}	D-H	H...A	D...A	∠DH...A
C1	H1	O1 ⁱⁱ	0.909(16)	2.567(17)	3.3846(19)	149.9(14)
C1	H1	O2 ^{vi}	0.909(16)	2.758(17)	3.428(2)	131.4(14)
C2	H2	O2 ⁱⁱⁱ	0.955(16)	2.606(16)	3.5473(19)	168.8(13)

^{a)} Symmetry codes: (ii) 1-x, -0.5+y, 0.5-z; (iii) -1+x, 0.5-y, -0.5+z; (vi) 1-x, -y, 1-z.

Packing of the layers is accompanied with Nitro/Nitro stacking, with each nitro group acting donor and acceptor of one such interaction

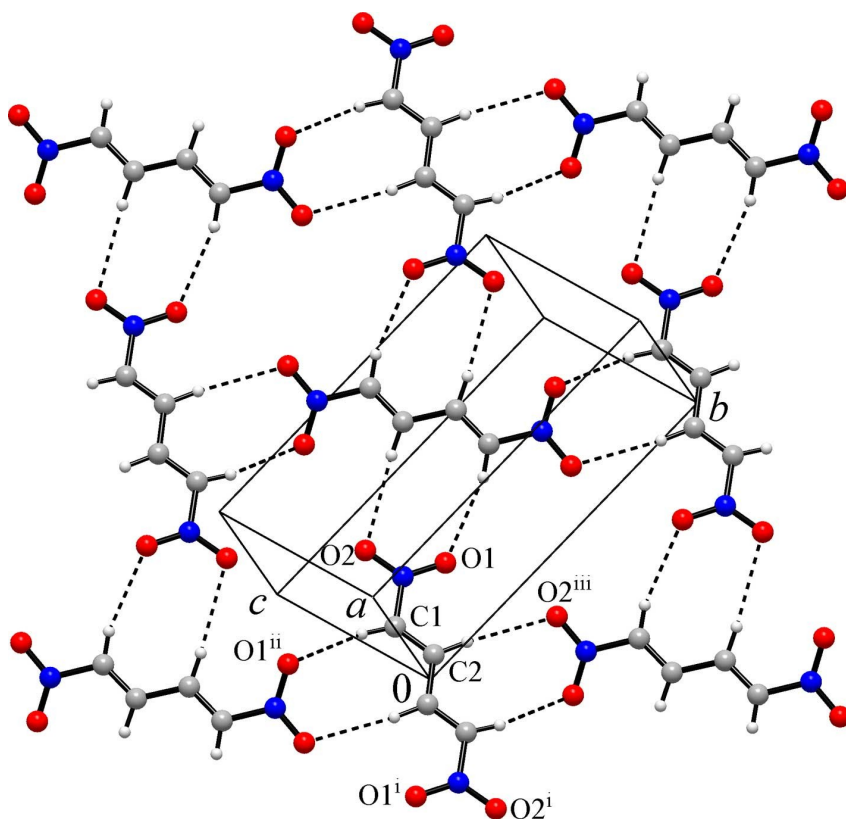


Figure S3. CH...O Hydrogen-bonded layer in the crystal structure of 1,4-dinitrobutadiene (**1**).

Symmetry codes: (ii) 1-x, -0.5+y, 0.5-z; (iii) -1+x, 0.5-y, -0.5+z.

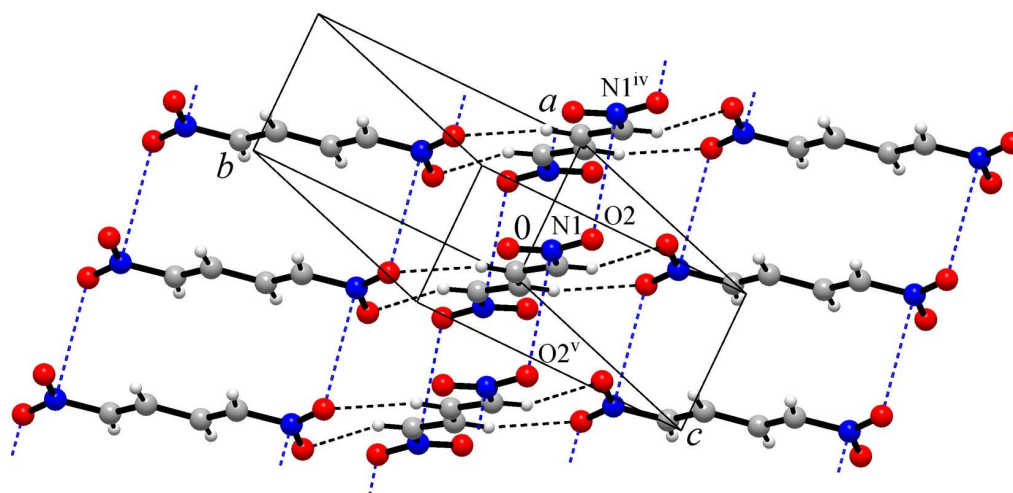


Figure S4. Nitro/Nitro interactions that occur between the CH \cdots O₂N bonded layers of 1,4-dinitrobutadiene molecules. Symmetry codes: (iv) $1+x, y, z$; (v) $-1+x, y, z$.

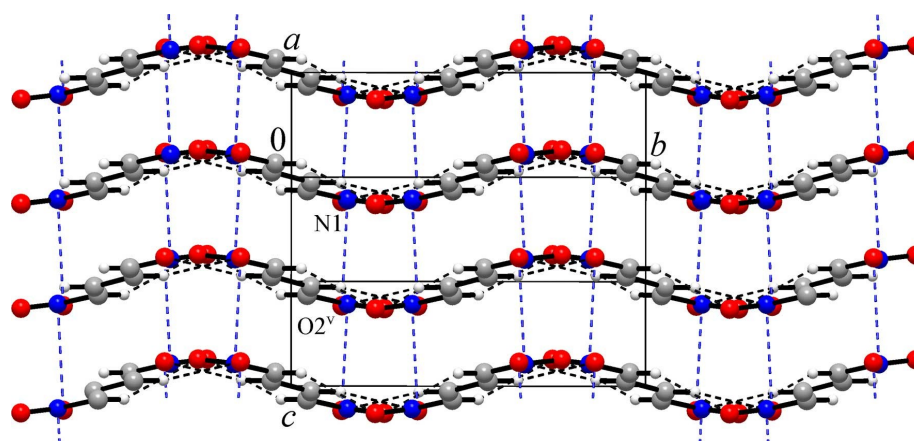


Figure S5. Packing of successive layers in the crystal structure of 1, showing the role of interlayer Nitro/Nitro interactions. Symmetry code: (v) $-1+x, y, z$.

3.2. Structure of 1,4-Dinitro-1,3-butadiene 1,4-dioxane solvate (**1a**)

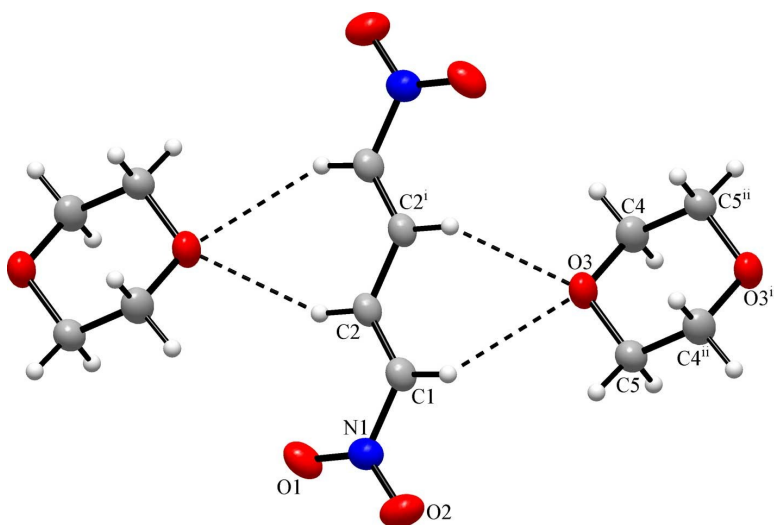


Figure S6. Molecular structure of 1,4-dinitro-1,3-butadiene 1,4-dioxane solvate (**1a**), with the thermal ellipsoids at 45% probability level. Symmetry codes: (i) $-x, 1-y, -z$; (ii) $1-x, 2-y, -z$.

In the crystal, configuration of 1,4-dinitrobutadiene molecules is identical to that in the structure of **1** (*trans-trans*-). Molecules of both components of the adduct reside across centers of inversion. Most noticeable intermolecular interactions in the structure are double CH \cdots O (Diox) bonding (Fig. S6), Nitro/Nitro and Nitro/O (Diox) bonding.

1,4-Dioxane, which is much stronger H-bond acceptor than nitro-group, provides rupture of CH \cdots O₂N pattern seen in **1**. Thus dioxane replaces NO₂ in the environment of the butadiene fragment and it establishes two CH \cdots O bonds (Table S2) with double C1-H1/C2ⁱ-H2ⁱ donors. Withdrawal of CH groups from the interactions with NO₂ groups facilitates more efficient interactions between nitro group themselves, as indicated by significant shortening of corresponding N \cdots O contacts (2.9145(10) Å for **1a** vs. 3.296(2) Å for **1**). Moreover, with elimination of weak H-bonding of NO₂ group, the structure defining role of Nitro/Nitro interactions is apparently increased. These interactions assemble the dinitrobutadiene molecules into the flat layers (square nets), which are parallel to the *bc* plane (Fig. S7) and each NO₂ group acts as donor and acceptor of one such interaction. At the same time, second axial side of NO₂ provides position for O₂N \cdots O interaction with dioxane (N \cdots O = 3.1620(11) Å), which terminates further possible Nitro/Nitro connectivity. Thus the dioxane molecules appear accommodated between the dinitrobutadiene layers by set of four CH \cdots O and two O₂N \cdots O bonds (Fig. S8).

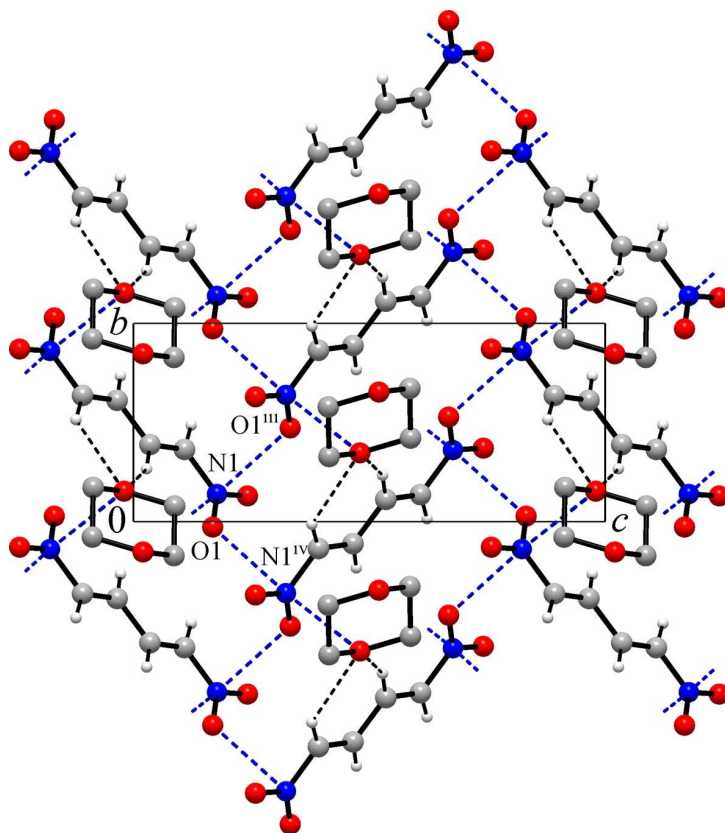


Figure S7. Projection of the structure **1a** on the *bc* plane, showing layers of 1,4-dinitro-1,3-butadiene molecules, which are held by Nitro/Nitro interactions (blue dotted lines). The dioxane

molecules are accommodated by a combination of double CH...O bonds and O...Nitro interactions. Symmetry codes: (iii) $-x, 0.5+y, 0.5-z$; (iv) $-x, -0.5+y, 0.5-z$.

Table S2. Hydrogen-bond geometry (Å, °) for structure of **1a**.

Donor (D)	Hydrogen (H)	Acceptor (A) ^{a)}	D-H	H...A	D...A	∠DH...A
C1	H1	O3	0.937(14)	2.652(14)	3.4209(12)	139.7(10)
C2	H2	O3 ^{vi}	0.920(12)	2.548(13)	3.3678(12)	148.7(10)

^{a)} Symmetry codes: (vi) $-x, 1-y, -z$.

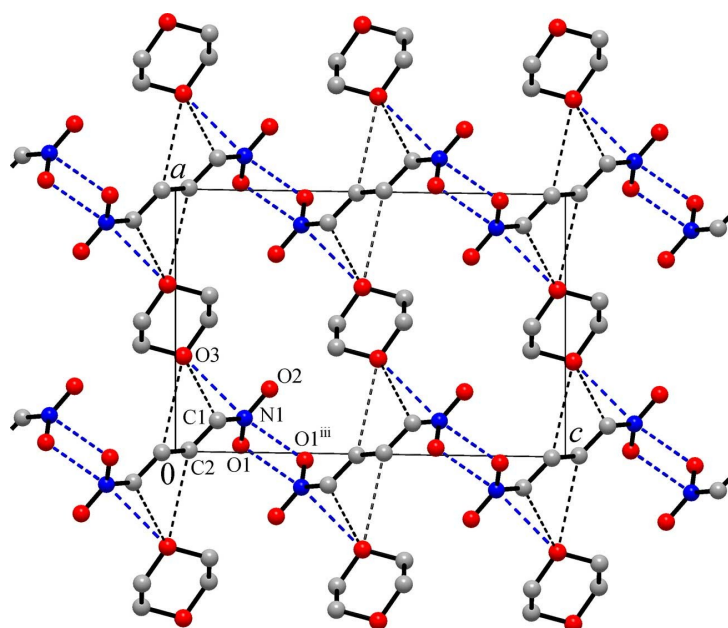


Figure S8. Projection of the structure **1a** on the *ac* plane: Function of dioxane molecules as links between layers of Nitro/Nitro bonded 1,4-dinitro-1,3-butadiene molecules (which are orthogonal to the drawing plane). Symmetry code: (iii) $-x, 0.5+y, 0.5-z$.

3.3. Structure of 1,4-Dinitro-1,3-pentadiene (**2**)

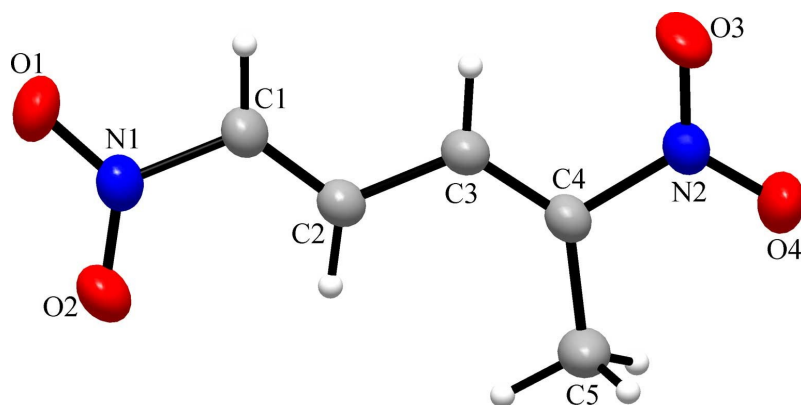


Figure S9. Molecular structure of 1,4-Dinitro-1,3-pentadiene (**2**), with the thermal ellipsoids at 45% probability level.

Molecules of the diene **2** reside in general positions and adopt the same configuration of the dinitrodiene skeleton as it was found for the unsubstituted butadiene analog **1**.

As may be compared with the structure of **1**, methylation eliminates one of the “double H-bond donor site” in the form of 1,3-(CH)₂ and the system is no more self-complementary (only one 1,3-(CH)₂ and two NO₂). Therefore, 2D H-bonded pattern seen in **1** is now disintegrated and H-bonding of the molecules yields discrete centrosymmetric dimers (Fig. S10). Further, interdimer, H-bonding is very weak, for example C...O separations for the

Table S3. Hydrogen-bond geometry (Å, °) for structure of **2**.

Donor (D)	Hydrogen (H)	Acceptor (A) ^a	D-H	H...A	D...A	∠DH...A
C1	H1	O3 ⁱ	0.967(15)	2.460(14)	3.2585(15)	139.8(11)
C2	H2	O1 ⁱⁱ	0.918(15)	2.691(15)	3.5804(15)	163.5(12)
C3	H3	O3 ⁱ	0.939(15)	2.670(15)	3.4368(15)	139.3(11)
C3	H3	O2 ^{viii}	0.939(15)	2.589(14)	3.2785(15)	130.5(11)
C5	H5A	O2 ^{vii}	0.98(2)	2.62(2)	3.4816(19)	147.3(15)
C5	H5B	O4 ⁱⁱⁱ	0.95(2)	2.79(2)	3.693(2)	159.2(17)
C5	H5C	O1 ⁱⁱ	0.99(2)	2.71(2)	3.6630(18)	161.7(15)

^a) Symmetry codes: (i) $-x, -y, -z$; (ii) $1.5-x, 0.5+y, -0.5-z$; (iii) $-x, 1-y, -z$; (vii) $-0.5+x, 0.5-y, 0.5+z$; (viii) $-1+x, y, z$.

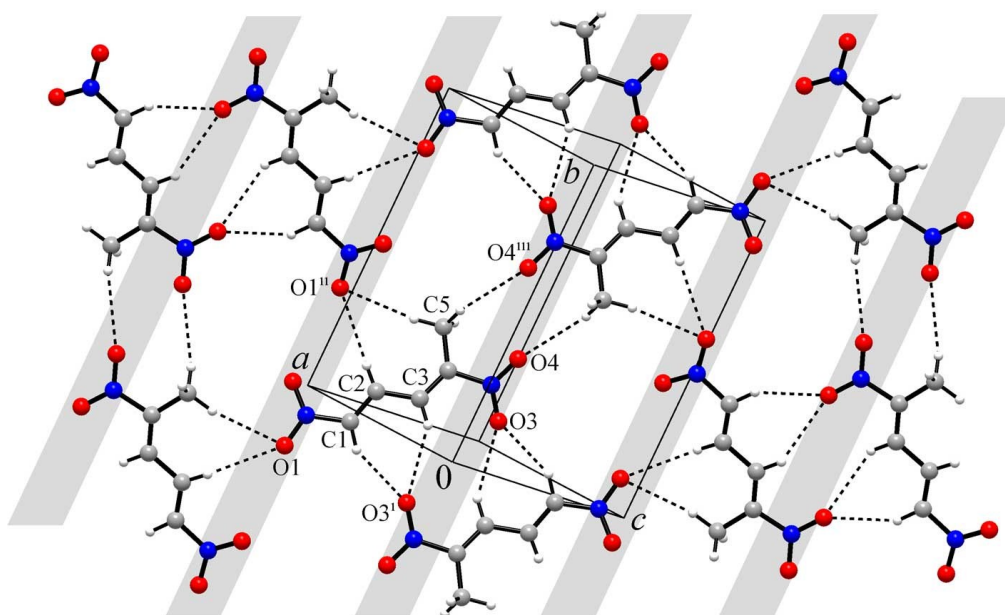


Figure S10. Fragment of the structure of 1,4-Dinitro-1,3-pentadiene (**2**), showing principal weak CH...O bonding. Symmetry codes: (i) $-x, -y, -z$; (ii) $1.5-x, 0.5+y, -0.5-z$; (iii) $-x, 1-y, -z$. The grey strips indicate non-covalent layers (which are orthogonal to the drawing plane) sustained with Nitro/Nitro interactions (See also Fig. S12, for simplified packing view).

possible H-bond formed by the remaining olefinic C2-H2 donor are as long as 3.5804(15) Å (Table S3). This dimer establishes two symmetrically equivalent π -hole interactions involving the nitro group next to the methyl group, in sharp agreement with the MEP surface that shows the most positive π -hole in this group (Fig. S11).

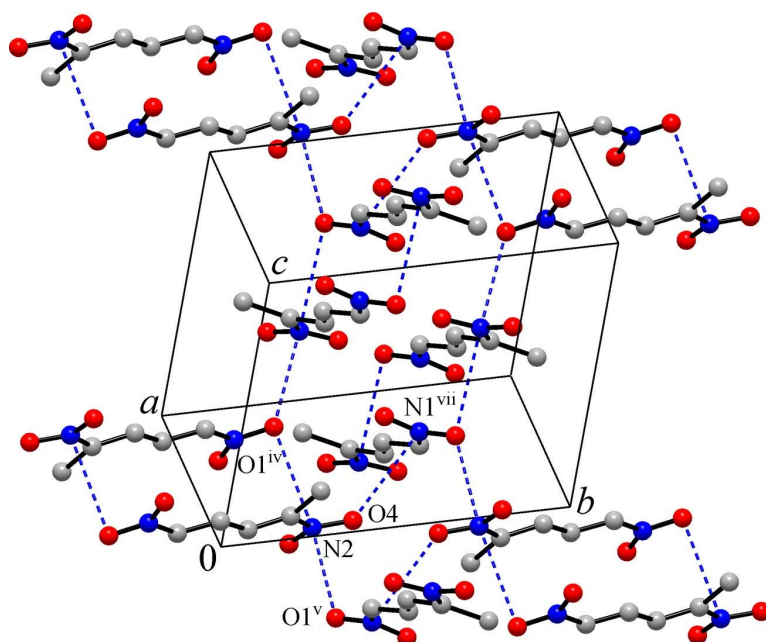


Figure S11. Fragment of the structure of 1,4-Dinitro-1,3-pentadiene (**2**), showing set of Nitro/Nitro interactions. Symmetry codes: (iv) $1-x, -y, -z$; (v) $0.5-x, 0.5+y, -0.5-z$; (vii) $-0.5+x, 0.5-y, 0.5+z$.

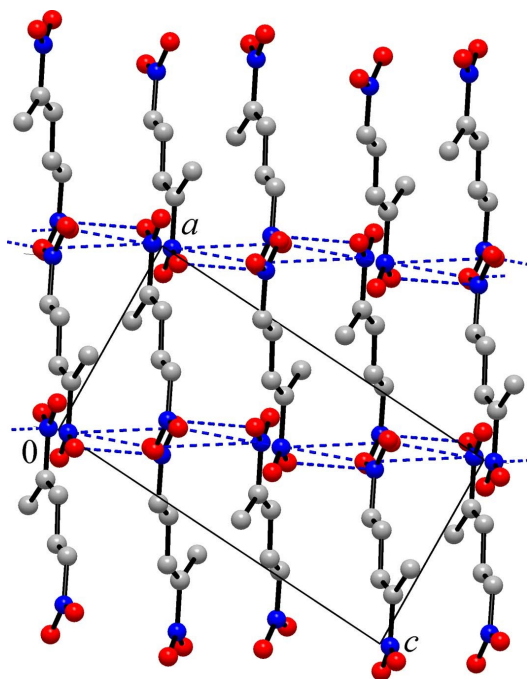


Figure S12. Projection of the structure of 1,4-Dinitro-1,3-pentadiene (**2**) on the *ac* plane: pentadien-1,3-diyl fragments as linkers between layers assembled by Nitro/Nitro interactions.

The NO₂/NO₂ bonding occurs between the successive “layers” of the weakly H-bonded molecules. The result may be viewed as layers of NO₂/NO₂ stacks, which are connected with covalent diene links –CH=CH–CH=C(Me)–, as it shown in Fig. 12. In this view, structure of the dinitropentadiene **2** is clearly a link between structures of unsubstituted butadiene **1** (dominant role of H-bonding) and structure of doubly methylated hexadiene **3** (dominated by Nitro/Nitro interactions): structural significance of both types of interactions is comparable and either H-bonded or Nitro/Nitro-stacked arrays are distinguishable supramolecular motifs.

3.4. Structure of 2,4-Dinitro-2,4-hexadiene (**3**)

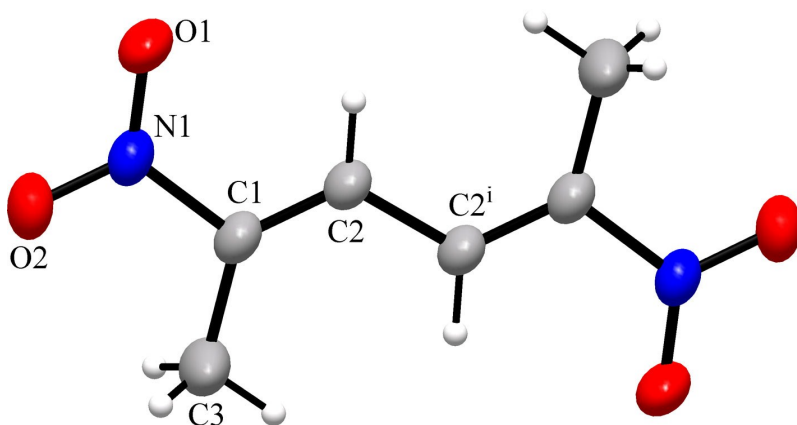


Figure S13. Molecular structure of 2,4-Dinitro-2,4-hexadiene (**3**), with the thermal ellipsoids at 45% probability level. Symmetry code: (i) 1–x, –y, –z.

Molecule of 2,4-dinitro-2,4-hexadiene adopts trans-trans-configuration and resides across a center of inversion (Fig. S13). Recently, we have demonstrated that the *cis/trans* relationships of this diene skeleton were also fully maintained in the cycloadducts formed with diazomethane (A.V. Sharko, et al., *Tetrahedron Lett.* **2015**, 56, 6089-6092).

Progressive methylation, as it was provided by evolution of **1** to **2** and **2** to **3**, results in elimination of “double H-bond donors” in the form of 1,3-CH. With the absense of such favorable sites in the structure of **3**, role of H-bonding decreases and there is only one very weak H-bond interaction, C2-H2...O1ⁱⁱ (symmetry code: (ii) 1.5–x, –0.5+y, 0.5–z), H2...O1ⁱⁱ = 2.733(19) Å; C2...O1ⁱⁱ = 3.583(2) Å; C2-H2...O1ⁱⁱ = 152.2(14)°. Instead, significance of Nitro/Nitro interactions is appreciable and the present structure is the most illustrative in this concern.

The nitro groups act as self-complementary double donors and acceptors of such interactions, which thus occur at both axial sides of NO₂ and engage each of the oxygen atoms. The corresponding separations are relatively short (N...O = 2.9615(18) and 3.1304(18) Å, Table S1) and the interactions are very directional, as is indicated by nearly orthogonal situation of the

O...N axes to the plane of the nitro groups ($79.5(2)$ and $84.3(2)^\circ$), and two N...O vectors are actually collinear: $O1^{iii}\cdots N1\cdots O2^{iv} = 171.5(2)^\circ$ (Fig. S14).

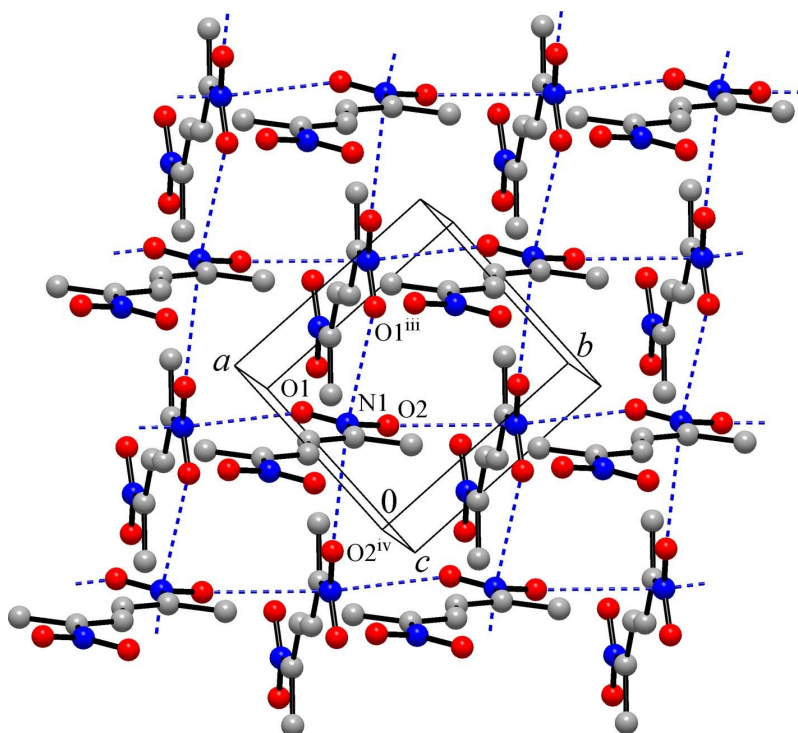


Figure S14. 2,4-Dinitro-2,4-hexadiene (**3**): 2D square net sustained entirely by Nitro/Nitro bonding (blue dotted lines), with the nitro groups as self-complementary donors and acceptors of two such interactions. Symmetry codes: (iii) $1.5-x, 0.5+y, 0.5-z$; (iv) $0.5-x, -0.5+y, 0.5-z$.

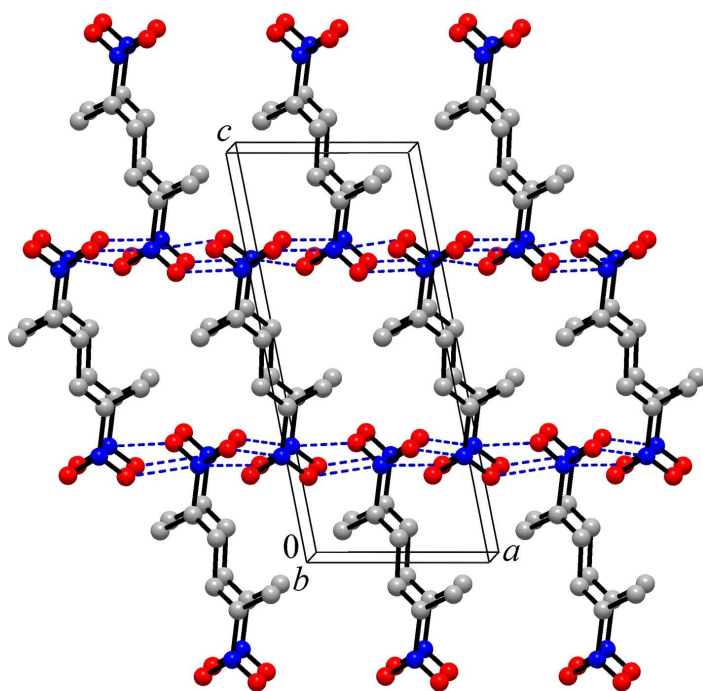


Figure S15. 2,4-Dinitro-2,4-hexadiene (**3**): 3D five-connected net, with hexane-2,4-diyl spacers as simple links between Nitro/Nitro connected non-covalent layers.

Thus, Nitro/Nitro stacking in **3** may be considered as a primary supramolecular force, which is responsible for production of the clear net topology. Hexadiene-2,4-diyl spacers interconnect 2D square layers sustained by Nitro/Nitro interactions (depicted in Fig. S14) giving rise five-connected 3D framework (See Fig. S15).

3.5. Computational methods

The energies of all complexes included in this study were computed at the RI-MP2/def2-TZVP level of theory. We have used the crystallographic coordinates for the theoretical analysis of the noncovalent interactions present in the solid state. The calculations have been performed by using the program TURBOMOLE version 7.0.ⁱ The interaction energies were calculated with correction for the basis set superposition error (BSSE) by using the Boys-Bernardi counterpoise technique.ⁱⁱ The Bader's "Atoms in molecules" theory has been used to study the interactions discussed herein by means of the AIMall calculation package.ⁱⁱⁱ The calculations for the wavefunction analysis have been performed at the MP2/def2-TZVP level of theory by means of the Gaussian09 calculation package.^{iv}

ⁱ R. Ahlrichs, M. Bär, M. Hacer, H. Horn and C. Kömel, *Chem. Phys. Lett.*, **1989**, *162*, 165–169.

ⁱⁱ S. B. Boys and F. Bernardi, *Mol. Phys.*, **1970**, *19*, 553–566.

ⁱⁱⁱ AIMall (Version 13.05.06), Todd A. Keith, TK Gristmill Software, Overland Park KS, USA, **2013**.

^{iv} Gaussian 09, Revision B.01, M. J. Frisch, G. W. Trucks, H. B. Schlegel, G. E. Scuseria, M. A. Robb, J. R. Cheeseman, G. Scalmani, V. Barone, G. A. Petersson, H. Nakatsuji, X. Li, M. Caricato, A. Marenich, J. Bloino, B. G. Janesko, R. Gomperts, B. Mennucci, H. P. Hratchian, J. V. Ortiz, A. F. Izmaylov, J. L. Sonnenberg, D. Williams-Young, F. Ding, F. Lipparini, F. Egidi, J. Goings, B. Peng, A. Petrone, T. Henderson, D. Ranasinghe, V. G. Zakrzewski, J. Gao, N. Rega, G. Zheng, W. Liang, M. Hada, M. Ehara, K. Toyota, R. Fukuda, J. Hasegawa, M. Ishida, T. Nakajima, Y. Honda, O. Kitao, H. Nakai, T. Vreven, K. Throssell, J. A. Montgomery, Jr., J. E. Peralta, F. Ogliaro, M. Bearpark, J. J. Heyd, E. Brothers, K. N. Kudin, V. N. Staroverov, T. Keith, R. Kobayashi, J. Normand, K. Raghavachari, A. Rendell, J. C. Burant, S. S. Iyengar, J. Tomasi, M. Cossi, J. M. Millam, M. Klene, C. Adamo, R. Cammi, J. W. Ochterski, R. L. Martin, K. Morokuma, O. Farkas, J. B. Foresman, and D. J. Fox, Gaussian, Inc., Wallingford CT, **2016**.